THE JOURNAL OF BIOLOGICAL CHEMISTRY

Vol. 265, No. 13, Issue of May 5, pp. 7455-7463, 1990
Printed in U.S.A.

A New Concept of Fibrin Formation Based upon the Linear Growth of Interlacing and Branching Polymers and Molecular Alignment into Interlocked Single-stranded Segments*

(Received for publication, July 11, 1989)

Ernst B. Hunziker‡, P. Werner Straub§, and André Haeberli§

From the M. E. Müller Institute for Biomechanics, University of Berne, Murtenstrasse 35, Berne CH-3010, Switzerland and the §Department of Internal Medicine, Inselspital, University of Berne, Berne CH-3010, Switzerland

In a previous electron microscopic study of early fibrin polymers processed by freeze drying and rotatory shadowing, a large proportion of loosely constructed, frequently branching linear molecular chains was observed; their structural organization was inconsistent with a half-staggered double-stranded model for fibrin polymerization. These conflicting results prompted us to investigate the structure of early fibrin polymers prepared according to a large variety of methods currently used for electron microscopy of macromolecules. By use of a systematic random sampling procedure, fibrin polymers were photographically recorded. They were classified according to their morphological form, and the frequency of occurrence of each configuration was determined. Half-staggered double-stranded forms accounted for less than 1% of all types encountered. Interpretation of the structural organization manifested in the diverse polymer forms observed necessitated the construction of a new interlocked single-strand model for fibrin polymerization.

The fibrin polymerization process combines simultaneous propagation of linear growth, branching, and lateral interlocking (leading to lateral association), resulting in the rapid formation of a fibrin network. The structural pattern developing during growth of fibrin polymers appears to be determined principally by the enzymatic mechanism and not solely by the intrinsic molecular structure of fibrinogen.

The validity of the interlocked single-strand model was tested by selective fibrinopeptide-B-releasing experiments. Under such activation conditions, the polymer forms predicted according to this and the half-staggered double-strand models should differ; the structures observed were indeed consistent with the interlocked single-strand hypothesis. The compatibility of existing data with this model is discussed.

Fibrinogen is a plasma glycoprotein that appears as a trinodular structure (~46 nm in length) consisting of a central E- and two peripheral D-domains in the electron microscope. The molecule is dimeric, each half being comprised of three polypeptide chains (Aα, Bβ, and γ) that are organized into helical strands between the domains. Thrombin converts fibrinogen to fibrin by cleaving off two fibrinopeptides-A and two fibrinopeptides-B. The fibrin monomers generated interact immediately, and thus the polymerization process is propagated. The fibrous network ultimately formed represents the structural basis for blood clot formation.

The early fibrin polymerization process is generally believed to follow the half-staggered double-strand (HSDS)[1] model proposed hypothetically by Ferry (1952) more than 35 years ago. However, recent observations made on early fibrin polymers prepared by cryotechnical processing and rotatory shadowing (Hunziker *et al.*, 1985, 1988) have revealed that the arrangement of fibrin molecules within early polymers is inconsistent with this proposal.

Structural requirements of a fibrin monomer necessary to account for the polymerization pattern observed (Hunziker *et al.*, 1985, 1988) include 1) intrinsic flexibility of the triple helical strands linking each nodule (see also Beijbom *et al.*, 1988); 2) radial symmetry of interaction sites through the E-domain (see also Dietler *et al.*, 1986); and 3) localization of either polymerization (on E) or binding (on D) sites on protruding chains (2-3 nm in length). It appears, moreover, that fibrin molecules within these early polymers are only partially activated, *i.e.* they exist as AB_2-fibrin (Alkjaersig and Fletcher, 1983; Dietler *et al.*, 1986; Hunziker *et al.*, 1988; Smith, 1980).

We suspected that the inconsistency of our findings with those of other investigators who have examined early fibrin polymer structure by transmission electron microscopy might originate from differences in preparation procedures, respecting not only the technique *per se* but also refinements of a particular protocol. Hence, in this investigation we have systematically analyzed and quantitated the structural features characterizing early fibrin polymers prepared according to a number of techniques currently adopted for electron microscopy of macromolecules.

In order to account for the observations made, it has been necessary to formulate a new model for fibrin polymerization based upon an interlocked single-strand (ISS) mechanism. The practicability of this and the HSDS model has been tested according to the unique predictions implicit to each

* This work was supported by Swiss National Science Foundation Grants 3.058-0.84 (to E. B. H.), 3.373-0.86, and 31-26500.89 (to P. W. S., A. H., and E. B. H.), by the Sandoz Foundation (Basel, Switzerland), and by the Roche Research Foundation (Basel). The costs of publication of this article were defrayed in part by the payment of page charges. This article must therefore be hereby marked "*advertisement*" in accordance with 18 U.S.C. Section 1734 solely to indicate this fact.

‡ To whom correspondence should be sent: M. E. Müller Institute for Biomechanics, University of Berne, P. O. Box 30, Berne CH-3010, Switzerland. Tel: 031-64-86-86; Fax: 031-25-02-59.

[1] The abbreviations used are: HSDS, half-staggered double strand; ISS, interlocked single strand; AB_2-, B_2-, and A_2-fibrin are generated after cleavage of one or both fibrinopeptides-A and both fibrinopeptides-B, respectively, from fibrinogen; a fibrin monomer unit is the building block of a growing fibrin polymer and may represent either AB_2-, B_2-, or completely activated fibrin; PPACK, D-phenylalanyl-L-prolyl-L-arginine chloromethyl ketone; HPLC, high pressure liquid chromatography.

respecting the configuration of polymers produced after selective removal of fibrinopeptide-B. The new ISS model is discussed in the light of previous experimental data interpreted according to the HSDS model.

MATERIALS AND METHODS

Rationale Behind Experiments

Methods currently used for visualizing macromolecules in the electron microscope all have in common a drying step. This is a critical preparative phase since it may affect the structural appearance of labile supramolecular assemblies. Hence, the following procedures were adopted: 1) air drying (at ambient temperature); 2) vacuum drying (at ambient temperature); and 3) freeze drying (at sub-zero temperatures).

Another critical phase is adhesion of molecules to the supporting stratum. This was performed either by immersion of mica plates in the polymer solution or by spraying this solution onto the supporting material. In the latter instance, strong shearing forces set up upon molecular contact could possibly affect polymer structure.

A third parameter that may influence and/or alter polymer structure is the chemical environment. Fibrin polymers were prepared in the absence or presence of glycerol and at physiological or high buffer-salt concentrations. Glycerol is generally added to polymer solutions prior to rotatory shadowing in order to improve stability and contrast (decoration effect) (Walzthöny *et al.*, 1981; Winkler *et al.*, 1985), and a hyperosmotic environment is frequently used in physicochemical studies on fibrin polymerization (Bale *et al.*, 1982, 1984; Mihalyi, 1988). A procedure that is particularly prone to producing artifacts is negative staining. Polymers are subjected twice to an air-drying process and hence to uncontrollable pH conditions and salt concentrations.

Outline of Experimental Procedures

Fibrin polymers were prepared by limited activation of fibrinogen with thrombin, the reaction being terminated by addition of PPACK. They were separated from reactants on a Sepharose CL-4B column and then diluted in isotonic or hypertonic buffer-salt media. Polymers were immediately processed for electron microscopic analysis according to a number of preparative procedures for rotatory shadowing or negative staining. They were sampled according to a random procedure (Cruz-Orive and Weibel, 1981), and each form counted was classified. The number of polymers/category was determined for each experimental condition, which was repeated between one and three times.

The role of fibrinopeptide-A release was assessed by activating fibrinogen with reptilase, which cleaves off this peptide exclusively (Blombäck, 1958; Landis, and Waugh, 1975). The specific role of fibrinopeptide-B release in fibrin polymerization was investigated using *Agkistrodon contortrix* venom as activating enzyme, which cleaves off preferentially fibrinopeptide-B from fibrinogen (this being achieved by its more rapid removal than fibrinopeptide-A (Blombäck *et al.*, 1978). The specificity of this enzyme, assessed by HPLC, was found to be approximately 70% (for fibrinopeptide-B cleavage). Since activation with this enzyme results in the release of approximately 30% fibrinopeptide-A, an alternative approach was also adopted. Prolonged activation of fibrinogen with thrombin was carried out in the presence of the tetrapeptide Gly-Pro-Arg-Pro, which has a high affinity for binding sites on D-domains. Under these conditions, α-chain-directed interactions between fibrin monomer units are prevented. In both types of experiments relating to selective removal of either fibrinopeptide-A or -B, fibrin polymers were prepared for electron microscopy by rapid freezing (in the absence of glycerol) and freeze drying.

Biochemical Procedures and Sample Preparation

Tris buffer (50 mM Tris-HCl, 0.1 M NaCl, pH 7.4) was used as incubation medium in all experiments and in final polymer solutions employing isotonic buffer-salt conditions. In hyperosmotic media, the sodium chloride concentration was raised to 0.25 M.

Human fibrinogen (Imco, Stockholm, Sweden) was further purified prior to experimental use by running it through a column of Sepharose CL-4B (Pharmacia LKB Biotechnology Inc.) to eliminate contaminating (2–5%) high molecular weight aggregates always present in commercial preparations.

Activation of fibrinogen (2.5–4.0 mg/ml) was achieved using thrombin (Hoffmann-La Roche) (0.005 NIH units/ml of fibrinogen solution), reptilase (Pentapharm, Basel, Switzerland) (0.06 Batroxobin units/ml of fibrinogen solution), or purified *A. contortrix* venom (Pentapharm) (1 μg/ml of fibrinogen solution). Using thrombin and reptilase as activating enzymes, incubations were carried out for 40–60 min at 20 °C. In the case of *A. contortrix* venom, prolonged incubation conditions (120 min at 20 °C) were adopted. Prolonged activation with thrombin (0.02 NIH units/ml of fibrinogen solution) was carried out for 100–120 min at 20 °C in the presence of the polymerization inhibitor Gly-Pro-Arg-Pro (at a final concentration of 1 mM). Enzyme activity was fully inhibited by addition of PPACK (Calbiochem) (at a final concentration of 0.5 μM). Aliquots of each incubation mixture were taken for fibrinopeptide-A and -B analysis by reversed-phase liquid chromatography (RP-column, Pharmacia). At the concentration of PPACK used, enzyme activity was fully blocked in each case.

Fibrin polymers were separated from fibrinogen by gel filtration on a Sepharose CL-4B column (100 × 2.6 cm). The early eluting fractions containing only fibrin polymers were used for electron microscopy. Aliquots from all fractions were diluted to 5 μg/ml in Tris buffer (prepared in the absence or presence of 40% (v/v) glycerol) and adsorbed onto mica plates (see below).

The extent of fibrin polymer activation within each column fraction was determined by radioimmunoassay as described previously (Hoffmann and Straub, 1977).

Electron Microscopy

Freeze Drying—This procedure has been described in detail previously (Hunziker *et al.*, 1988) and is only summarized here.

Polymer adhesion to freshly cleaved mica (Ruby B, Wachendorf, Basel, Switzerland) was achieved either by spraying solutions directly onto this surface or by immersing the mica plates in polymer solutions. After a few seconds to allow for polymer adsorption, mica plates were immersed in liquid nitrogen (maintained at −196 °C) for rapid cryofixation. Polymer solutions destined for "spraying" were prepared in isotonic buffer-salt media in the absence or presence of glycerol (final concentration, 40% (v/v)); those destined for "immersion" were prepared either in iso- or hypertonic buffer-salt media in the absence of glycerol (see Table I). Frozen specimens were inserted into a magnetic freeze-dry table (Balzers, Lichtenstein) and stored in liquid nitrogen prior to further processing. The table was then placed on a precooled stage (−130 °C) of a Balzers' 360 M freeze etching device for freeze drying at −180 °C for 30 min and at −30 °C for an additional 60 (±10) min under a vacuum of 4 (±2) × 10^{-7} millibars. Rotatory shadowing was performed (using platinum/carbon) at an elevation angle of 10° and by rotating the table at approximately 100 turns/min. The platinum/carbon film was backed with pure carbon fired from an angle of 80–90°. Film thicknesses were monitored by quartz oscillators and recorded to be 1.5 nm (platinum/carbon) and 10–15 nm (carbon). The shadowed mica plates were thawed at room temperature and maintained in a water-saturated atmosphere for 48 h prior to the removal of platinum/carbon films by flotation on bidistilled water. These were then lifted free upon 400-mesh copper grids for examination in the electron microscope.

Vacuum Drying—Vacuum drying was carried out according to conventional protocols, *i.e.* polymer solutions were prepared in the presence of 40% (v/v) glycerol (final concentration). Both isotonic (spraying and immersion) and hypertonic (immersion only) buffer-salt environments were employed (see Table I). Polymers adhered to mica plates were vacuum dried for 3 h at 5 (±2) × 10^{-6} millibars prior to shadowing (see "Freeze Drying").

Air Drying—Fibrin polymers were prepared exclusively in glycerol-containing (final concentration, 40% (v/v)) isotonic buffer-salt solutions. They were adsorbed onto mica plates (either by spraying or immersion; see Table I) and then air dried at ambient temperature (20 °C) prior to shadowing (see "Freeze Drying").

Negative Staining—Polymers, prepared in either isotonic or hypertonic buffer-salt solutions, were adsorbed onto glow-discharged carbon films (supported on copper grids) by immersion. These films were air dried at ambient temperature and then immersed briefly in 2% (w/v) uranyl acetate solution (aqueous). They were again air dried prior to examination in the electron microscope.

Examination of Fibrin Polymers—All specimens were examined either in a Philips 301 or 400 electron microscope operated at 60 kV and with 40- or 70-μm aperture diaphragms, respectively. Specimen carrier films were supported on 400-mesh copper grids and electron micrographs of polymers taken within grid squares according to a

systematic random sampling procedure (Cruz-Orive and Weibel, 1981). Polymer forms were classified according to shape, eight different configurations being observed (see Fig. 4). The number of forms counted varied between 403 and 626/experimental condition (see Table I).

RESULTS

All morphological configurations observed, either for a segment within a branching fibrin polymer or for the polymer as a whole (when uniform in structure), are illustrated in Figs. 1–4; the relative frequencies at which each form is encountered under the various experimental conditions are represented in Table I. In order to avoid confusion, the rationale behind the naming of each category is not given at this juncture. The significance of each term will, however, become apparent under "Discussion."

The form most frequently observed under all experimental conditions (in the range of 66.5–86.4%) is the *loose longitu-*

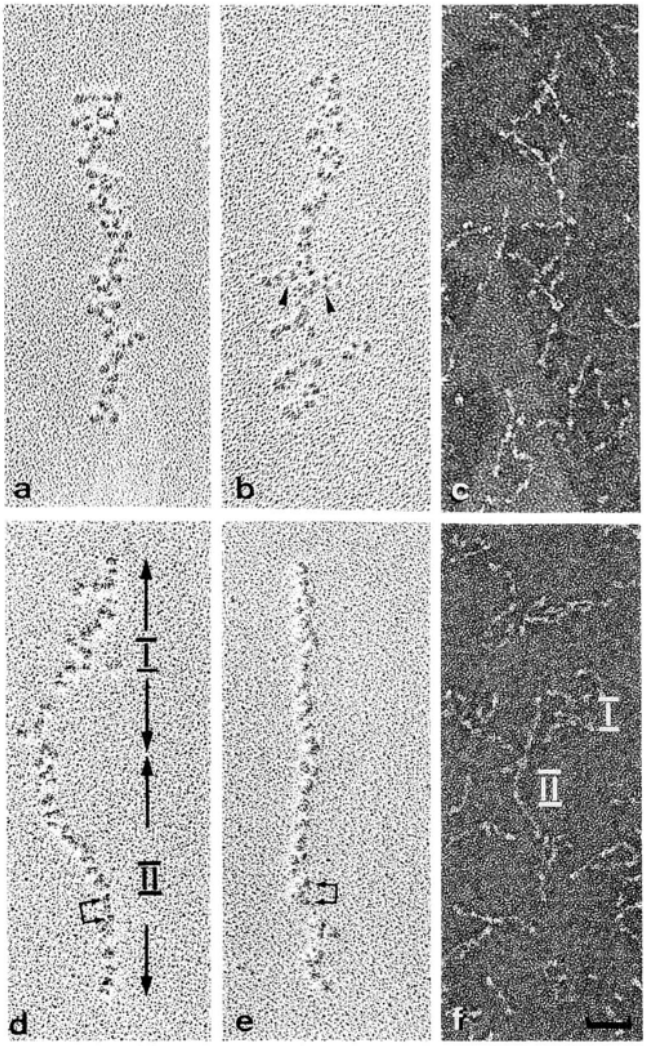

FIG. 1. *a–c*, electron micrographs of loose longitudinal aggregates (see Fig. 4*I*). This polymer form is characterized by linear growth along the main longitudinal axis, with respect to which incorporated fibrin monomer units are randomly orientated. Branching (see, for example, ▲ in *b*) occurs frequently within these polymers. *d* and *f*, electron micrographs of early fibrin polymers undergoing molecular alignment. In *segment I*, individual molecules are only partially activated (*i.e.* to AB_2-fibrin) and are thus still randomly oriented relative to the main axis. In the remaining segment (*II*), activation (with respect to fibrinopeptide-A release) has been completed, and B_2-fibrin molecules are consequently aligned into a single strand (see Fig. 4*II*). *e*, electron micrograph of a polymer exhibiting complete alignment into a single strand. It is characterized by a repeating α,γ-linked trinodular unit of 23 nm (*arrow pair*) each domain of which is derived from a different molecule (see Figs. 7 and 8 for diagrammatic representation). *a, b, d,* and *e*, molecules rotatory shadowed with platinum/carbon; *c* and *f*, molecules negatively stained with uranyl acetate. Magnification, × 120,000; *bar*, 50 nm.

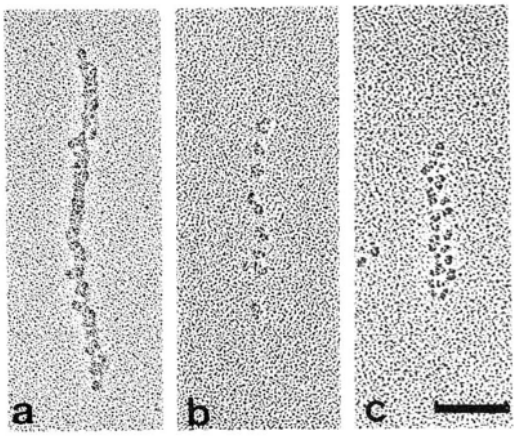

FIG. 2. **Electron micrographs of fibrin polymers with *a*, interlocked double-strand (see Fig. 4*III*); *b*, end-to-end single-strand (see Fig. 4*VI*); and *c*, half-staggered double-strand (see Fig. 4*VII*) configurations.** Molecules rotatory shadowed with platinum/carbon. Magnification, × 100,000; *bar*, 100 nm.

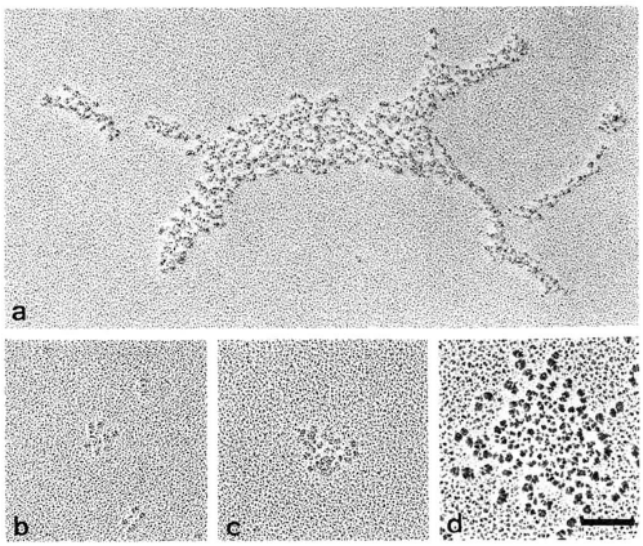

FIG. 3. *a*, electron micrograph of a fibrin cluster obtained after activating fibrinogen with thrombin in the presence of the tetrapeptide Gly-Pro-Arg-Pro. Under these reaction conditions, α-chain-directed interactions are prevented. The chain-like segments sometimes observed are most probably a consequence of small ordering effects resulting from nonspecific lateral associations. These compact multiple-layered polymer segments may also occur after thrombin activation in the absence of Gly-Pro-Arg-Pro and are referred to as interlocked multiple strands (see (Fig. 4*IV*). *b, c*, electron micrographs of fibrin polymers in which molecular domains are organized into loose clusters without an apparent axis of linear growth. Such polymers are included in the loose longitudinal aggregate category (see Fig. 4*I*). *d*, electron micrographs of fibrin clusters obtained after activating fibrinogen with *A. contortrix* venom, which cleaves off predominantly fibrinopeptide-B. Fibrin monomer units form variably sized compact clusters with no sign of a regular aggregation pattern (see Fig. 6*c*, *II* for explanation). Such clusters may also be seen after thrombin activation and are classified as dense unordered aggregates (see Fig. 4*V*). Molecules rotatory shadowed with platinum/carbon. Magnification, × 70,000; *bar*, 100 nm. The *larger grain size* observed in *d* is attributable to a difference in shadowing conditions.

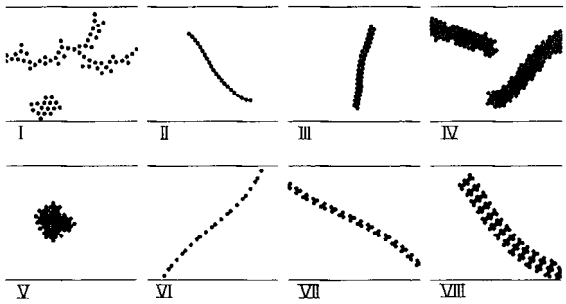

FIG. 4. **Schematic representation of examples from each fibrin polymer form category.** Fibrin polymer forms observed in the electron microscope are classified into eight categories: *I*, loose longitudinal aggregate; *II*, interlocked single strand; *III*, interlocked double strand; *IV*, interlocked multiple strand; *V*, dense unordered aggregate; *VI*, end-to-end single strand; *VII*, half-staggered double strand; *VIII*, half-staggered multiple strand.

dinal aggregate (Fig. 1, *a–c*; category I in Table I and Fig. 4). It comprised both discrete segments within and the entire structure of polymers, which were frequently and consistently branched. To this category belong also small polymers with domains organized into loosely packed clusters which do not (yet?) exhibit a linear axis of growth (Fig. 3, *b* and *c*). The second most frequently observed polymer form (in the range of 3.1–19.5%) is the *interlocked single strand* (Fig. 1*e*; category II in Table I and Fig. 4), which is characterized by single linear chains of densely packed molecular domains. Such strands commonly occur as segments within loose longitudinal aggregates (Fig. 1, *d* and *f*). Two other categories that share in common with the interlocked single strand a dense packing of domains along the linear polymer axis are *interlocked double* (Fig. 2*a*; category III in Table I and Fig. 4) and *interlocked multiple* (Fig. 3*a*; category IV in Table I and Fig. 4) *strands*. Their frequencies of occurrence lie within the ranges of 0.4–5.2% and 0–5.8%, respectively (Table I). Configuration category V includes the *dense unordered aggregates* (Figs. 3*d* and 4), which consisted of molecular domains densely packed into clusters without an apparent axis of linear growth. This form is encountered within a frequency range of 1–17.5% (Table I). Polymer category VI consists of *end-to-end single strands*, which correspond to fibrin monomer units arranged end to end along a single axis (Figs. 2*b* and 4). This form occurred almost exclusively as very short segments within loose longitudinal aggregates and seldom as the only structural component of an entire polymer. It was encountered within a frequency range of 0–13.4% (Table I). Category VII corresponds to the *half-staggered double-strand* polymer form so frequently described in the literature (Figs. 2*c* and 4). It occurred with a frequency in the range of 0.4–2% (Table I). A *half-staggered multiple-strand* form (category VIII in Table I and Fig. 4) was observed in a single instance only (see Table I).

Of these eight polymer forms, only the last two, namely, the half-staggered double- and multiple-strand configurations, are consistent with the HSDS model hypothesis for fibrin polymerization. These represent less than 1% of all morphological forms observed. All other configurations, constituting more than 99%, are inconsistent with this model. In order to accommodate these findings, it has been necessary to construct a new model. This proposal (the ISS model hypothesis), characterized by linear growth, branching, and lateral association phenomena, occurring simultaneously from the onset of polymerization, is described under "Discussion."

A point that we wished to clarify respecting the reaction mechanism for this ISS model hypothesis was whether linear polymer growth, branching, and lateral association phenomena are dependent upon fibrinopeptide-B removal. The morphology of early fibrin polymers (prepared according to cryotechnical procedures) was examined after activation of fibrinogen with either thrombin (which cleaves off both fibrinopeptides-A and -B) or reptilase (which selectively removes fibrinopeptides-A (Blombäck, 1958; Landis and Waugh, 1975). The profile distribution for each polymer form category was identical in each case, indicating that the mechanism by which linear polymer growth, branching, and lateral association occur is independent of fibrinopeptide-B removal.

According to predictions made commensurate with either the HSDS or ISS model hypotheses, fibrin polymer forms produced by selective removal of fibrinopeptide-B from fibrinogen should differ (see Figs. 5 and 6 and "Discussion"). This selective activation condition may be achieved using *A. contortrix* venom, which cleaves off ~70% of fibrinopeptide-B and ~30% of fibrinopeptide-A (determined by HPLC; see "Materials and Methods" and Blombäck *et al.*, 1978). An alternative approach is to add an excess of the tetrapeptide Gly-Pro-Arg-Pro during prolonged thrombin activation. By so doing, the molecular interaction that depends upon fi-

TABLE I

Categorization of observed fibrin polymer forms

The number of polymer forms within each category (I–VIII) is expressed as a percentage of the total number analyzed (*n*) for each experimental condition in two to four separate investigations. The abbreviations used are: FD, freeze dried; VD, vacuum dried; AD, air dried; NS, negatively stained; −G, in the absence of glycerol; +G, in the presence of 40% (v/v) glycerol; S, spraying technique; I, immersion technique.

Preparation technique	No. of polymers analyzed	I Loose longitudinal aggregate	II Interlocked single strand	III Interlocked double strand	IV Interlocked multiple strand	V Dense unordered aggregate	VI End-to-end single strand	VII Half-staggered double strand	VIII Half-staggered multiple strand
	n					%			
FD/−G/S	403	80.0	9.1	1.8	2.7	4.6	1.3	0.5	0
FD/−G/I	495	86.4	3.3	5.2	2.1	1.0	0	2.0	0
FD/+G/S	469	78.9	8.4	1.1	3.4	7.7	0.1	0.4	0
FD/−G[a]/I	479	66.5	19.5	0.4	0.6	11.3	0.8	0.9	0
VD/+G/S	524	79.1	12.2	3.5	0.5	3.0	0.7	1.0	0
VD/+G/I	440	84.3	4.9	0.5	1.6	7.6	0.2	0.9	0
VD/+G[a]/I	626	66.7	14.6	1.2	3.7	12.1	1.3	0.4	0
AD/+G/S	430	79.4	4.2	1.0	5.2	9.4	0.3	0.5	0
AD/+G/I	530	66.6	3.1	4.5	5.8	17.5	0.6	1.7	0.2
NS/−G/I	442	68.6	9.0	1.0	0	6.4	13.0	2.0	0
NS/−G[a]/I	429	67.7	15.5	0.6	0	1.8	13.4	1.0	0

[a] High buffer-salt concentration.

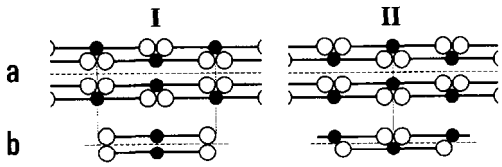

FIG. 5. **HSDS model hypothesis: theoretical predictions relating to aggregation patterns produced after selective removal of fibrinopeptides-B from fibrinogen (illustrations are represented as two-dimensional models).** *a*, fibrin monomer units polymerizing according to the half-staggered double-strand model under normal activation conditions. Such double-stranded fibrils could associate with one another either in register (*aI*) or in a half-staggered double-stranded manner (*aII*). If the former case was operative, then in the absence of α-chain-directed interactions, only single pairs of fibrin monomer units would form (*bI*); if fibrils associated in a half-staggered manner, then half-staggered pairs or longer double-chain segments would be produced (*bII*).

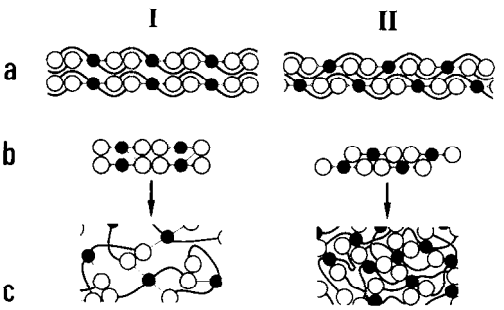

FIG. 6. **ISS model hypothesis: theoretical predictions relating to aggregation patterns produced after selective removal of fibrinopeptides-B from fibrinogen.** *a*, fibrin polymerization according to the interlocked single-strand model hypothesis under normal activation conditions. Such fibrils could associate laterally with one another either in register (*bI*) or in a half-staggered manner (*bII*). In the former case, selective removal of fibrinopeptide-B (in the absence of α-chain-directed interactions) would lead to the formation of loosely arranged clusters, with no direct contact being established between E- and D-domains involved in β-chain-directed interactions (*cI*). If fibrils associated laterally in a half-staggered manner, then selective removal of fibrinopeptide-B would yield compact dense clusters with direct domainal contact at interaction sites (*cII*).

brinopeptide-A removal is blocked (Laudano and Doolittle, 1980). The disadvantage here is that the importance of fibrinopeptide-B removal cannot be studied without cleaving off some fibrinopeptide-A. Furthermore, the Gly-Pro-Arg-Pro tetrapeptide also has an affinity (although this is low) for fibrinopeptide-B-dependent binding sites (Laudano and Doolittle, 1980).

Activation by *A. contortrix* venom yields irregularly shaped dense clusters of variable size (Fig. 3*d*) with little sign of longitudinal growth except in a small proportion of fibrin polymers (presumably containing larger amounts of AB_2-fibrin). The cluster formation is even more pronounced after prolonged thrombin activation in the presence of the tetrapeptide Gly-Pro-Arg-Pro, these appearing larger and more densely packed (Fig. 3*a*). The polymer forms produced in each instance are consistent with predictions made according to the ISS model hypothesis (see "Discussion"). Although fibrin polymer clusters showed variation in packing density in these experiments, the domains of individual fibrin monomer units were observed to contact neighboring nodules directly, without spatial separation. This is indicated by the shadowing effect produced, *i.e.* apparent reduced domainal size and lack of background grain in the center of these clusters (see Fig. 3*d*). Thus, neither the polymerization (on E) nor the binding (on D) sites (Budzynski, 1986; Olexa and Budzynski, 1980) exposed after fibrinopeptide-B cleavage appear to be located on a protruding chain (see Fig. 6*c*, *I* and *II*) unless the length of this lies below the resolution limits of the technique applied (*i.e.* less than 2 nm).

DISCUSSION

The early fibrin polymers formed during activation of fibrinogen are labile structures that exist in dynamic equilibrium with the reacting molecules (Bale *et al.*, 1985; Blombäck *et al.*, 1981; Dietler *et al.*, 1985, 1986; Hunziker *et al.*, 1985, 1988; Janmey *et al.*, 1983a; Scheraga, 1983; Sturtevant *et al.*, 1955). Associations between constituent fibrin monomer units are formed by interaction of polymerization sites located near the N terminus of α-chains on central E-domains (Laudano and Doolittle, 1978, 1980; Olexa and Budzynski, 1980) with binding sites located near the C terminus of γ-chains on peripheral D-domains (Horwitz *et al.*, 1984; Olexa and Budzynski, 1980; Váradi and Scheraga, 1986). These interactions are weak (Ferry *et al.*, 1954; Laudano and Doolittle, 1978, 1980; Scheraga, 1983), and hence it would not be surprising if they were partially or completely disrupted under certain preparative conditions used in electron microscopic studies. In most previous investigations, HSDS polymer forms (categories VII and VIII in Table I and Fig. 4) have been described after specimen preparation in the presence of high salt concentrations followed by negative staining or rotatory shadowing (Fowler *et al.*, 1981; Hantgan *et al.*, 1980, 1983). In a recent report of ours (Hunziker *et al.*, 1988), early fibrin polymers prepared strictly according to cryotechniques were described as being inconsistent with the HSDS model for fibrin polymerization. In an endeavor to determine whether methodologically induced artifacts were responsible for these conflicting results, we applied a large number of preparative procedures currently used in electron microscopic studies of macromolecules. The resulting polymer forms were sampled according to a systematic random procedure, classified (see Fig. 4), and quantitated (see Table I).

Fibrin Polymer Configurations—Loose longitudinal aggregates made up the vast majority of species observed in the electron microscope under all experimental conditions, including negatively stained molecules and those prepared at high salt concentrations (see Table I). These loosely associated linear aggregates, together with the interlocked single-, double-, and multiple-strand polymer forms and dense unordered aggregates (categories I–V in Table I and Fig. 4) do not conform with the HSDS model for fibrin polymer growth. The morphological diversity encompassed within these five categories suggests that fibrin polymers exhibit preferential rather than exclusive linear growth combined with frequent and simultaneous branch formation and lateral association.

Interlocked Single-strand Model Hypothesis for Fibrin Polymerization—Since loosely associated longitudinal aggregates constitute the highest proportion of polymer species encountered, this form most probably represents an early stage in the polymerization process. The single-stranded configuration, in which domains are densely organized (interlocked single strand; category II in Table I and Fig. 4), frequently existed as segments within the loosely associated longitudinal aggregates, and as such, they may be indicative of a secondary alignment process.

The models represented in Fig. 7 illustrate the sequence of events that we believe to occur during molecular alignment within early fibrin polymers. This process is most likely a consequence of further activating fibrin monomers from the AB_2- (in loosely associated longitudinal aggregates) to the B_2-form (in interlocked single strands). Removal of this second

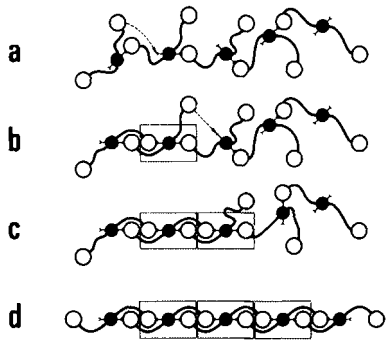

FIG. 7. **Two-dimensional representation of the alignment process within a fibrin polymer segment.** *a*, loose longitudinal aggregate. This early fibrin polymer is characterized by the following features (see Hunziker *et al.*, 1988). 1) Incorporated fibrin monomer units retain the inherent flexibility of fibrinogen molecules; 2) the topographic location of polymerization and binding sites is characterized by radial symmetry; 3) either polymerization or binding sites are located on protruding peptide chains (2–3 nm in length); 4) incorporated fibrin monomers exist predominantly in the AB_2-activation state. Each incorporated AB_2-fibrin monomer unit is linked to two neighboring molecules, one via an E → D and the other via a D → E interaction, and this pattern of association leads to linear growth of fibrin polymers. Each AB_2-fibrin monomer unit is then further activated to B_2-fibrin by removal of its second fibrinopeptide-A, whereby the second binding site on the E-domain is exposed. This interacts with a neighboring D-domain (- - →) and marks the onset of the alignment process. Subsequent figures (*b–d*) illustrate how the process of molecular alignment proceeds until at completion, a single-stranded fibrin polymer segment (interlocked single strand) is produced (*d*), this being characterized by the repeating α,γ-linked trinodular unit. ○, peripheral D-domains of a fibrin monomer unit; ●, central E-domain of a fibrin monomer unit; ——; flexible, triple-helical chain of fibrin monomer unit; ——c, polymerization site located on peptide chain; ▭, demarcation of α,γ-linked trinodular units formed upon completion of molecular alignment.

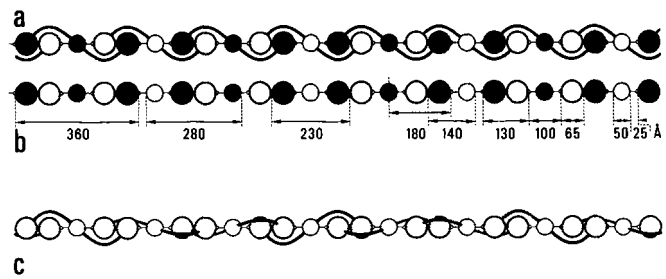

FIG. 8. **Two-dimensional representations of aligned interlocked single-stranded fibrin polymers.** *a*, complete model including triple-helical portions of fibrin monomer units, the domains of which are represented alternately as *filled* and *unfilled circles*. *b*, in this illustration, triple-helical bridges between the domains of a fibrin monomer unit have been omitted for the sake of clarity. The repeating signal of an α,γ-linked trinodular unit (230 Å) is indicated together with various other periodicities, some of which have been recorded after negative staining or x-ray diffraction of fibrin fibers (Kay and Cuddigan, 1967; Ruska and Wolpers, 1940; van Zandt Hawn and Porter, 1947; Weisel, 1986; Weisel *et al.*, 1987; Williams, 1983). The length of an individual fibrin monomer unit aligned within the polymer is ~360 Å. *c*, three-dimensional model of an aligned interlocked single-stranded fibrin polymer segment. The triple-helical portions linking molecular domains may twist to a certain degree and thus may be oriented at all points around the longitudinal axis.

fibrinopeptide-A exposes the other polymerization site on the E-domain (situated radially opposite the first near the N terminus of the α-chain (Hoeprich and Doolittle, 1983; Laudano and Doolittle, 1978, 1980; Olexa and Budzynski, 1980), which then interacts with the binding site on the neighboring D-domain (located near the C terminus of the γ-chain (Horwitz *et al.*, 1984; Olexa and Budzynski, 1980; Varadi and Scheraga, 1986) of an adjacent fibrin monomer unit). Hence, molecular alignment leads to the formation of DED-trinodular units, each domain of which originates from a different molecule. Since each trinodular unit is formed via an interaction between a polymerization and binding site located on α- and γ-chains, respectively, we refer to these structures as α,γ-linked trinodular units. Within such a unit, an interlocking interaction involving three different B_2-fibrin molecules is established, and the linear arrangement of these leads to the formation of interlocked single-strand segments. The formation of single-strand oligomers during fibrin polymerization has also been shown by use of a novel imaging method, *i.e.* the atomic force microscope (Drake *et al.*, 1989).

Based upon the measurements for D- (6.5 nm) and E- (5.0 nm) domain diameters and the length of the chain on which polymerization and binding sites are located (2–3 nm), an α,γ-linked trinodular unit may be calculated to be 23 (±1) nm in length (*i.e.* (2 × 6.5 (D)) + 5.0 (E) + (2 × 2.5 (E-D binding)) nm). Since neighboring α,γ-linked trinodular units occur immediately adjacent to one another, the alignment process would be consistent with the periodic signal of 23 nm (Fig. 8) found previously in negatively stained fibrin fibrils and fibers (Hewat *et al.*, 1982; Kay and Cuddigan, 1967; Ruska and Wolpers, 1940; van Zandt Hawn and Porter, 1947; Weisel, 1986; Weisel *et al.*, 1983; Williams, 1981). In morphological appearance, the α,γ-linked trinodular unit resembles the trinodular fibrinogen molecule except that its length is reduced by half. The linear domain density (*i.e.* number of domains/unit length) for an aligned ISS polymer segment would thus be equivalent to that achieved across the *two* strands in the HSDS model.

Polymerization Mechanism—The HSDS model was constructed in the belief that it was necessary to explain linear polymer growth of a molecule possessing two polymerization and two binding sites that were activated simultaneously. It was assumed that such a molecule was stiff and that its interaction sites were organized in a top–bottom fashion (initial complete activation of molecules in which polymerization and binding sites were characterized by radial symmetry, would inevitably lead to cluster formation). As such, it would be the imposed structural constraints that forced fully activated molecules to grow linearly in double strands; single-strand polymer growth would not be possible.

In contrast, molecular flexibility and radial symmetry of interaction sites serve as the basis for the ISS model. According to this proposal, initial activation of both polymerization sites would lead to cluster formation; the preferential linear growth observed would be accounted for by "monofunctional activation," *i.e.* activation of only one polymerization site at a time (note that the two binding sites on D are continually ready for interaction and do not require activation) to yield the AB_2-fibrin form (as encountered in loose longitudinal aggregates). Indeed, previous studies have shown that the fibrinopeptide-releasing mechanism by thrombin really can be modulated (Lewis *et al.*, 1985; Mihalyi, 1988; Torbet, 1986; Vali and Scheraga, 1986). One possible mechanism by which monofunctional activation of fibrinogen molecules could be achieved is now discussed.

Following the removal of one fibrinopeptide-A from the E-domain of a fibrinogen molecule, the exposed polymerization site interacts immediately with the binding site on a D-domain of a neighboring fibrinogen molecule. Since binding sites are continually exposed on D-domains, *i.e.* thrombin activation is not required to prepare them for interaction, the initial dimer consists of one partially activated (*i.e.* AB_2-) fibrin monomer unit and one unactivated fibrinogen molecule. It is conceivable that this primary E → D interaction induces

(allosterically) a conformational change in the α-chain within the ipsilateral half of the unactivated fibrinogen molecule on which the D-domain has been contacted, such that the fibrinopeptide-A is here removed in preference to that from a free fibrinogen molecule (Alkjaersig *et al.*, 1983). This step would lead to the formation of a trimer, and propagation of this activation mechanism would thus lead to linear growth of the early labile fibrin polymers (Fig. 1, *a–c*).

Support for the Proposed Reaction Mechanism—It has been demonstrated previously that the polymerization process occurs much faster than fibrinogen activation by thrombin (Bale *et al.*, 1982; Janmey, 1982; Visser and Payens, 1982); these data would be satisfied by and offer support for the proposed reaction mechanism. It has also been shown that the removal of a second fibrinopeptide-A from a fibrinogen molecule occurs 16–40 times faster than cleavage of the first (Janmey *et al.*, 1983b; Landis and Waugh, 1975). It was assumed that the "second" fibrinopeptide-A was the second of the two located on a single AB_2-fibrin molecule. Interpretation of the second fibrinopeptide-A as one of those on the (A_2B_2-) fibrinogen molecule which has already interacted (via its D-domain) with the initial AB_2-fibrin monomer unit would also be consistent with these data and support the activation mechanism proposed here.

According to the Flory-Stockmayer theory (Flory, 1941, 1953; Stockmayer, 1943), early branching is a prerequisite for the polymerization and gelation process and, indeed, was frequently and consistently observed already in the labile unaligned fibrin polymers (loose longitudinal aggregates) produced during the initial stage of thrombin activation (Figs. 1*b* and 9). The length of fibrin polymers is not a critical factor in determining the onset of branching, in contrast to what was believed previously (Doolittle, 1984; Hantgan *et al.*, 1983). The mechanism by which it occurs is, moreover, independent of fibrinopeptide-B release, since the polymerization patterns produced by activating fibrinogen with reptilase (which cleaves off fibrinopeptide-A, exclusively) were identical to those observed after thrombin activation (see also Torbet, 1987). The basis for branching during the early stage of polymerization most likely lies in the occurrence of initial bifunctional activation of fibrinogen molecules to B_2-fibrin monomer units (Fig. 9). The frequency at which either a mono- or bifunctional activation occurs probably follows stochastic laws, and hence the activation mechanism itself determines the fibrin polymerization pattern, *i.e.* the extension of linear growth, the frequency of branching, lateral association (see below), and hence the rate of network formation. The localized occurrence of multiple bifunctional activation (corresponding perhaps to localized high thrombin activity or relatively low substrate concentration) would lead to unordered polymer growth and cluster formation. A situation such as this would account for the dense unordered aggregates regularly observed (Table I).

Branching could also occur during molecular alignment if a peripheral D-domain of an incorporated fibrin monomer unit interacts with a free and newly generated AB_2- or B_2-fibrin molecule (or with a neighboring aligning polymer) instead of being integrated into its own chain (see Figs. 10 and 11).

In addition to marking the onset of true branching, bifunctional activation could also lead to lateral association between branches and hence to further mechanical stabilization of fibrils and fibers (Fig. 11). Early branching within labile unaligned fibrin polymers may also be important in this respect.

Nonincorporated D-domains may also represent sites for lateral association between loose longitudinal aggregates by the interlocking of domains (Fig. 10). This phenomenon thus represents the third of the three basic mechanisms—namely, linear growth, branching, and lateral association—operating simultaneously during polymerization. Nonincorporated D-domains could also serve as sites for adhesion to cell surfaces (Fig. 11*f*), and there is indeed some evidence for this (Doolittle *et al.*, 1979; Plow *et al.*, 1985; Rixon *et al.*, 1983).

Test of Model Predictions—According to an old postulate (Laurent and Blombäck, 1958), fibrinopeptide-B-dependent interactions play a role only in secondary processes such as stabilization of (laterally) associated and aligned polymers in order to produce durable fibrils and fibers (Budzynski, 1986; Torbet, 1987). Indeed, our experiments relating to selective fibrinopeptide-A removal (by reptilase) showed that the early polymerization events (such as linear growth, branching, lateral association, and molecular alignment) are all independent of fibrinopeptide-B release. Predictions made respecting the mechanism by which fibrinopeptide-B (and thus β-chain)-dependent interaction takes place differ according to either the HSDS or ISS models. These were tested by morphological analysis of the fibrin polymer forms resulting from selective fibrinopeptide-B removal from fibrinogen.

Since binding sites exposed after fibrinopeptide-B removal

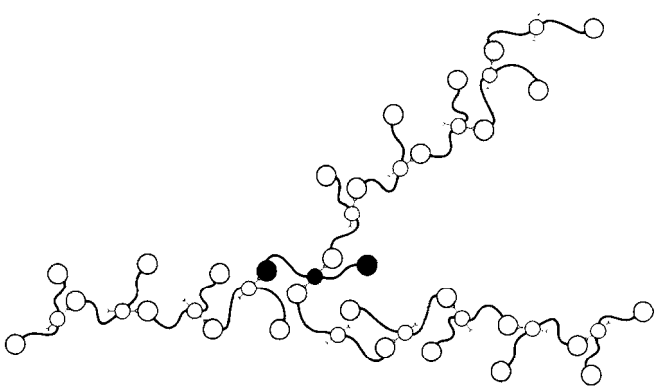

FIG. 9. **Two-dimensional representation of a branching loose longitudinal aggregate.** The molecule forming the point of bifurcation (represented in *black*) is believed to be fully activated with respect to fibrinopeptide-A release (*i.e.* to B_2-fibrin).

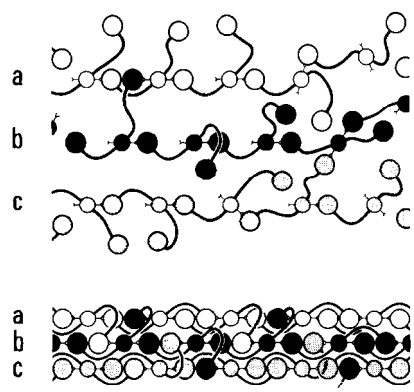

FIG. 10. Two-dimensional representation of a triple-stranded (*top, a–c*) loose longitudinal aggregate. Completion of the molecular activation process (with respect to fibrinopeptide-A release) here leads to further interaction among the three polymer chains via incorporation of D-domains into a neighboring rather than the parent branch. The three completely aligned polymer strands (*bottom, a–c*) are thus interlocked by stable lateral associations. To improve the clarity of the figure, helical portions between domains have not been drawn to scale; to emphasize the interdigitation effect among the three strands, domains of each are *shaded* differently (○, *a*; ●, *b*; ○, *c*; ◍, D-domain of a fourth strand (not shown) incorporated into branch *c*).

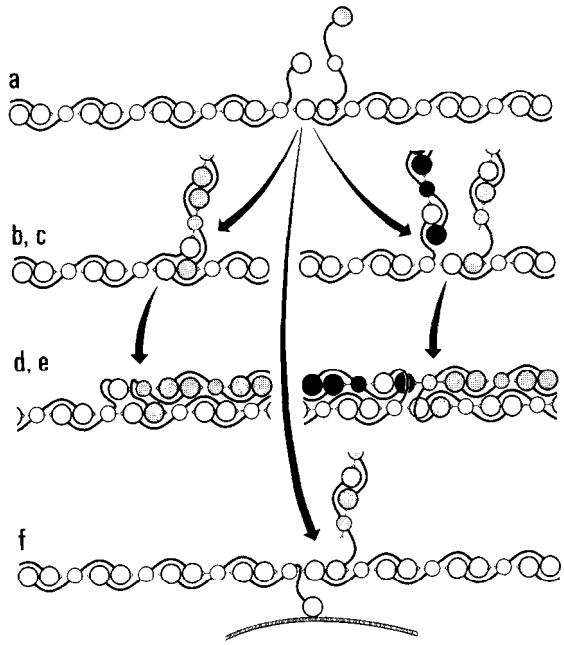

FIG. 11. **Two-dimensional representations of branching phenomena in interlocked single-stranded fibrin polymer segments.** One terminal D-domain of the fibrinogen molecule represented in *a* (with *speckled* domains) has become integrated into an aligned polymer strand as a consequence of initial activation of both polymerization sites on the E-domain of an incorporated fibrin monomer unit, and a branching point is thereby created. The D-domain of this fibrinogen molecule takes the place of that from an incorporated fibrin monomer unit that would have "normally" folded back into the chain during the alignment process. The latter domain is consequently free either to incorporate into the branch during its alignment (*b*), serve as a starting point for the development of a second branch (*c*), or remain unbound and represent a site for adhesion to cell surfaces (*f*). The branches represented in *b* and *c* may also fold back onto the parent strand, as shown in *d* and *e*, respectively, and their position here is stabilized by the formation of lateral associations between polymer segments (see Fig. 10).

FIG. 12. *a*, cross-section of aligned interlocked single-stranded fibrin fibrils associated by lateral contacts, illustrating a possibility for three-dimensional packing. Irrespective of internal twisting along the longitudinal fibril axis, such chains will always have the capacity for localized high spatial density packing, which would account for the high mechanical resistance known to characterize fibrin networks. At the same time, the model also allows for very low density regions (in which various plasma or tissue macromolecules may lodge during polymerization). The possibilities for variation in packing density, from very high to very low, compatible with this model thus account for the overall high mechanical resistance and low packing density measured for fibrin networks (Hermans, 1979). *b*, cross-section of half-staggered double-stranded fibrils associated by lateral contacts, illustrating a possible three-dimensional packing arrangement. In this case, optimal space filling cannot be achieved locally in space. Hence, the high mechanical resistance of fibrin networks is not accounted for in concurrence with an overall low fibrin density. Any internal twisting of double-stranded fibrils (Weisel, 1986) along their longitudinal axes is likely to decrease packing density further unless winding of the whole fiber axis occurs in synchrony (○, D-domain; ●, E-domain).

are not involved in linear growth of fibrin polymers, it seems unlikely that they are activated via a monofunctional mechanism (on the grounds that this is not required). Hence, using the ISS model as a working hypothesis, it may be predicted that fibrin polymers appear as disorganized aggregates of low stability, and this indeed was found to be the case (Fig. 3*a*). Furthermore, individual D- and E-domains appeared to contact one another directly (Fig. 6*c*, *II*), indicating that binding sites on β-chains are not located on protruding peptide chains unless these are shorter than 2 nm (the limit for lateral resolution).

According to the HSDS model for fibrin polymerization (Ferry, 1952; Stryer *et al.*, 1963), fibrinogen molecules exhibit axial symmetry, in which case β-chains would be arranged in parallel, *i.e.* located on the same side of an E-domain (see Hoeprich and Doolittle, 1983 for discussion). If this was so, (functional) A_2-fibrin monomers would be expected to associate consistently in rigid "ordered" pairs or in half-staggered double-stranded chain segments (as illustrated in Fig. 5), even in the absence of B_2-fibrin monomer interactions. Some chain-like structures (loose longitudinal aggregates) were apparent after fibrinogen activation with thrombin in the presence of Gly-Pro-Arg-Pro, but these most likely arise as a consequence of nonspecific effects of this tetrapeptide upon fibrinopeptide-B-dependent interactions (Fig. 3*a*). The occurrence of a proportion of linear polymer segments when using *A. contortrix* venom as activating enzyme is to be expected on the grounds of its low specificity and thus a result of fibrinopeptide-A removal, which permits linear growth. However, short ordered pairs or half-staggered double strands were never observed under either of these activation conditions. The results provide evidence for the ISS model and, indirectly, for the radially symmetrical organization of fibrinopeptide-B-dependent interaction sites on fibrinogen.

The lateral association pattern of ISS chains during fibril formation most likely corresponds to that depicted in Fig. 6*a*, *II*, in which two single-stranded fibrin polymers are illustrated. In space, such fibrin polymers may be surrounded by six neighboring ones (see Fig. 12), thus providing the basis for high variability in packing density and hence in the extent to which other molecules are incorporated (Galanakis *et al.*, 1987; Torbet, 1986) while still retaining considerable mechanical stability of fibrin fibers.

The new model accords well with data published previously. In contrast to the HSDS model, no inconsistencies have been revealed when using the ISS model as a working hypothesis.

Acknowledgments—We are indebted to Ceri England for the English correction of the manuscript and to B. Rindlisbacher and M. Wullschleger for technical assistance. We are grateful to W. Herrmann, W. Hess, and R. Ambrosi for their help with the artwork.

REFERENCES

Alkjaersig, N., and Fletcher, A. P. (1983) *Biochem. J.* **213,** 75–83
Bale, M. D., Janmey, P. A., and Ferry, J. D. (1982) *Biopolymers* **21,** 2265–2277
Bale, M. D., Janmey, P. A., Ferry, J. P., and Laurent, L. (1984) *Biopolymers* **23,** 127–138
Bale, M. D., Müller, M. F., and Ferry, J. D. (1985) *Proc. Natl. Acad. Sci. U. S. A.* **82,** 1410–1413
Beijbom, L., Larsson, U., Kaveus, U., and Hebert, H. (1988) *J. Ultrastruct. Mol. Struct. Res.* **98,** 312–319
Blombäck, B. (1958) *Ark. Kemi* **12,** 321–335
Blombäck, B., Hessel, B., Hogg, D., and Therkildsen, L. (1978) *Nature* **275,** 501–505
Blombäck, B., Hessel, B., Okada, M., and Egberg, N. (1981) *Ann. N. Y. Acad. Sci.* **370,** 536–544
Budzynski, A. Z. (1986) *CRC Crit. Rev.* **6,** 97–146
Cruz-Orive, L. M., and Weibel, E. R. (1981) *J. Microsc. (Oxford)* **122,** 235–257
Dietler, G., Känzig, W., Haeberli, A., and Straub, P. W. (1985) *Biochemistry* **24,** 6701–6706
Dietler, G., Känzig, W., Haeberli, A., and Straub, P. W. (1986) *Biopolymers* **25,** 905–929
Doolittle, R. F. (1984) *Annu. Rev. Biochem.* **53,** 195–229

Doolittle, R. F., Watt, K. W. K., Cottrell, B. A., Strong, D. D., and Riley, M. (1979) *Nature* **280,** 464–468
Drake, B., Prater, C. B., Weisenhorn, A. L., Gould, S. A. C., Albrecht, T. R., Quate, C. F., Cannell, D. S., Hansma, H. G., and Hansma, P. K. (1989) *Science* **243,** 1586–1589
Ferry, J. D. (1952) *Proc. Natl. Acad. Sci. U. S. A.* **38,** 566–569
Ferry, J. D., Katz, S., and Tinoco, I., Jr. (1954) *J. Polym. Sci. Part D Macromol. Rev.* **12,** 509–516
Flory, P. J. (1941) *J. Am. Chem. Soc.* **63,** 3083–3100
Flory, P. J. (1953) *Principles of Polymer Chemistry*, Cornell University Press, Ithaca, NY
Fowler, W. E., Hantgan, R. R., Hermans, J., and Erickson, H. P. (1981) *Proc. Natl. Acad. Sci. U. S. A.* **78,** 4872–4876
Galanakis, D. K., Lane, B. P., and Simon, S. R. (1987) *Biochemistry* **26,** 2389–2400
Hantgan, R. R., Fowler, W. E., Erickson, H., and Hermans, J. (1980) *Thromb. Haemostasis* **3,** 119–124
Hantgan, R. R., McDonagh, J., and Hermans, J. (1983) *Ann. N. Y. Acad. Sci.* **408,** 344–366
Hermans, J. (1979) *Proc. Natl. Acad. Sci. U. S. A.* **76,** 1189–1193
Hewat, E. A., Tranqui, L., and Wade, R. H. (1982) *J. Mol. Biol.* **161,** 459–477
Hoeprich, P. D., Jr., and Doolittle, R. F. (1983) *Biochemistry* **22,** 2049–2055
Hoffmann, V., and Straub, P. W. (1977) *Thromb. Res.* **11,** 171–181
Horwitz, B. H., Varadi, A., and Scheraga, H. A. (1984) *Proc. Natl. Acad. Sci. U. S. A.* **81,** 5980–5984
Hunziker, E. B., Haeberli, A., and Straub, P. W. (1985) *Thromb. Haemostasis* **54,** 2 (abstr.)
Hunziker, E. B., Haeberli, A., and Straub, P. W. (1988) *J. Ultrastruct. Mol. Struct. Res.* **98,** 60–70
Janmey, P. A. (1982) *Biopolymers* **21,** 2253–2264
Janmey, P. A., Bale, M. D., and Ferry, J. D. (1983a) *Biopolymers* **22,** 2017–2019
Janmey, P. A., Erdile, L., Bale, M. D., and Ferry, J. D. (1983b) *Biochemistry* **22,** 4336–4340
Kay, D., and Cuddigan, B. J. (1967) *Br. J. Haematol.* **13,** 341–347
Landis, W. J., and Waugh, D. F. (1975) *Arch. Biochem. Biophys.* **168,** 498–511
Laudano, A. P., and Doolittle, R. F. (1978) *Proc. Natl. Acad. Sci. U. S. A.* **75,** 3085–3089
Laudano, A. P., and Doolittle, R. F. (1980) *Biochemistry* **19,** 1013–1019
Laurent, T. C., and Blombäck, B. (1958) *Acta Chem. Scand.* **12,** 1875–1881
Lewis, S. D., Shields, P. P., and Shafer, J. A. (1985) *J. Biol. Chem.* **260,** 10192–10199
Mihalyi, E. (1988) *Biochemistry* **27,** 976–982
Olexa, S. A., and Budzynski, A. Z. (1980) *Proc. Natl. Acad. Sci. U. S. A.* **77,** 1374–1378
Plow, E. F., Pierschbacher, M. D., Ruoslahti, E., and Marguerie, G. A. (1985) *Proc. Natl. Acad. Sci. U. S. A.* **82,** 8057–8061
Rixon, M. W., Chan, W.-Y., Davie, E. W., and Chung, D. W. (1983) *Biochemistry* **22,** 3237–3244
Ruska, H., and Wolpers, C. (1940) *Klin. Wochenschr.* **19,** 695
Scheraga, H. A. (1983) *Ann. N. Y. Acad. Sci.* **408,** 330–343
Smith, G. F. (1980) *Biochem. J.* **185,** 1–11
Stockmayer, W. H. (1943) *J. Chem. Phys.* **11,** 45–55
Stryer, L., Cohen, C., and Langridge, R. (1963) *Nature* **197,** 793–794
Sturtevant, J. M., Laskowski, M., Jr., Donnely, T. H., and Scheraga, H. A. (1955) *J. Am. Chem. Soc.* **77,** 6168–6172
Torbet, J. (1986) *Biochemistry* **25,** 5309–5314
Torbet, J. (1987) *Biochem. J.* **244,** 633–637
Vali, Z., and Scheraga, H. A. (1988) *Biochemistry* **27,** 1956–1963
van Zandt Hawn, C., and Porter, K. R. (1947) *J. Exp. Med.* **86,** 285–297
Váradi, A., and Scheraga, H. A. (1986) *Biochemistry* **25,** 519–528
Visser, A., and Payens, T. A. (1982) *FEBS Lett.* **142,** 35–38
Walzthöny, D., Moor, H., and Gross, H. (1981) *Ultramicroscopy* **6,** 259–266
Weisel, J. W. (1986) *J. Ultrastruct. Mol. Struct. Res.* **96,** 176–188
Weisel, J. W., Phillips, G. N., Jr., and Cohen, C. (1983) *Ann. N. Y. Acad. Sci.* **408,** 367–379
Weisel, J. W., Nagaswami, C., and Makowski, L. (1987) *Proc. Natl. Acad. Sci. U. S. A.* **84,** 8991–8995
Williams, R. C. (1981) *J. Mol. Biol.* **150,** 399–408
Williams, R. C. (1983) *Proc. Natl. Acad. Sci. U. S. A.* **80,** 1570–1573
Winkler, H., Wildhaber, J., and Gross, H. (1985) *Ultramicroscopy* **16,** 331–339

A new concept of fibrin formation based upon the linear growth of interlacing and branching polymers and molecular alignment into interlocked single-stranded segments.

E B Hunziker, P W Straub and A Haeberli

J. Biol. Chem. 1990, 265:7455-7463.
